

Partial Motion Imitation for Learning Cart Pushing with Legged Manipulators

Mili Das^{1*}, Morgan Byrd¹, Donghoon Baek¹, and Sehoon Ha¹

Abstract—Loco-manipulation is a key capability for legged robots to perform practical mobile manipulation tasks, such as transporting and pushing objects, in real-world environments. However, learning robust loco-manipulation skills remains challenging due to the difficulty of maintaining stable locomotion while simultaneously performing precise manipulation behaviors. This work proposes a partial imitation learning approach that transfers the locomotion style learned from a locomotion task to cart loco-manipulation. A robust locomotion policy is first trained with extensive domain and terrain randomization, and a loco-manipulation policy is then learned by imitating only lower-body motions using a partial adversarial motion prior. We conduct experiments demonstrating that the learned policy successfully pushes a cart along diverse trajectories in IsaacLab and transfers effectively to MuJoCo. We also compare our method to several baselines and show that the proposed approach achieves more stable and accurate loco-manipulation behaviors.

I. INTRODUCTION

Legged robots have recently demonstrated increasingly capable locomotion and manipulation skills in real-world environments [1], [2], [3]. In particular, legged manipulators—quadrupedal robots with manipulators mounted on top—offer a promising solution for mobile manipulation tasks in unstructured factory or home environments, such as transporting objects and assisting with everyday activities. Among these tasks, pushing everyday objects, like carts, is especially relevant for practical automation scenarios, including warehouse logistics and retail environments. Successful deployment in these settings requires coordinated loco-manipulation behaviors that maintain stable locomotion while simultaneously generating accurate manipulation forces over long time horizons.

However, learning robust loco-manipulation policies remains challenging. Recent approaches often rely on automated frameworks, such as deep reinforcement learning, to discover coordinated whole-body behaviors. These methods typically require extensive reward engineering and meticulous training design. The simpler task of learning stable locomotion alone often involves a large number of reward terms, sometimes exceeding 10 to 20 components, alongside extensive domain randomization to achieve robust performance across diverse environments. Extending these approaches to loco-manipulation further increases the complexity of policy learning and naively combining locomotion and manipulation objectives often leads to unstable or inefficient solutions.

To address these complexities, we draw inspiration from self-imitation. Recent motion imitation approaches have

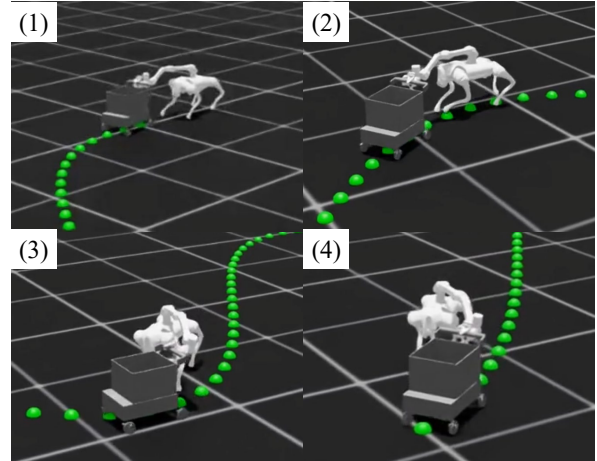


Fig. 1: Cart loco-manipulation along a predefined path (green dotted curve). The robot initiates contact at (1), performs straight pushing and coordinated turning maneuvers (2–4), continuously adjusting whole-body coordination to maintain stable contact and balance while tracking the target trajectory.

shown promising results in humanoid [4] and quadrupedal control problems [5]. However, such methods typically rely on large-scale reference datasets, which are not available for loco-manipulation tasks. Existing datasets, such as OMOMO [6], focus primarily on full-body human motions and are not directly applicable to legged loco-manipulation. Instead, we propose to imitate the locomotion style that emerges from a simpler task and transfer it to the more complex setting of loco-manipulation. Specifically, we preserve the lower-body motion patterns that produce stable locomotion while allowing the arm to adapt freely to the manipulation task.

This paper presents a novel framework for learning a robust loco-manipulation policy using partial imitation learning. We first learn a locomotion policy on rough terrain. At this stage, the locomotion policy is trained with extensive domain and terrain randomization to obtain robust and transferable walking behaviors. We then train a loco-manipulation policy by imitating only the lower-body motions using an adversarial motion prior (AMP) [7], which preserves the locomotion style while allowing the arm to learn effective manipulation behaviors. Our key insight is that full-body imitation would unnecessarily constrain manipulation behaviors, yet learning without imitation often results in unstable locomotion because the policy must simultaneously discover locomotion and manipulation strategies. By imitating only the lower-body motions, the learned policy maintains stable locomotion while enabling effective manipulation and can be combined with a standard path-following controller to push

¹Georgia Institute of Technology, Atlanta, GA, 30308, USA

*Correspondence to mdas45@gatech.edu

a cart along desired trajectories.

We evaluate the proposed learning framework on a cart loco-manipulation task and observe consistently stable and reliable performance, while assuming reliable cart position estimation. When combined with a widely adopted high-level path-following controller, the learned policy successfully tracks a variety of trajectories in the IsaacLab simulation environment over long time horizons. The policy also transfers effectively across simulators, demonstrating successful sim-to-sim transfer from IsaacLab to MuJoCo. Compared to baseline approaches without imitation or with full-body imitation, our method achieves significantly improved performance and stability.

The main contributions of this work are:

- We propose a novel partial imitation learning approach for robust legged loco-manipulation.
- We demonstrate stable cart loco-manipulation through extensive simulation experiments, including strong performance in the training environment (IsaacLab) and successful sim-to-sim transfer (MuJoCo).
- We show that the proposed approach outperforms baseline methods, including policies trained without imitation, with full-body imitation, and hierarchical RL.

II. RELATED WORKS

A. *Quadrupedal Locomotion*

Model-based approaches are one of the key methodologies for solving quadrupedal locomotion. To do this, they typically use model-predictive control formulations that solve simplified rigid-body dynamics online at high rates [8], [9], [10], [11]. These methods are appealing as they offer interpretable behavior and stability guarantees. However, they depend on accurate dynamics models and predefined contact schedules, limiting robustness on unstructured terrain with unknown surface properties.

Learning-based methods address these limitations by training robust policies in simulation with extensive domain randomization and transferring them to hardware [12], [13], [14], [15], [16]. Along with improving robustness via domain randomization, these methods also attempt to handle the partial observability of key state information, e.g. dynamics and terrain properties, at test time. Dominant strategies include teacher-student distillation of privileged terrain information [14], [17] and online adaptation modules that infer latent environment parameters from the proprioceptive history [18], [19], [20]. Our work follows the proprioception-only, domain-randomized paradigm to train a reference locomotion policy, whose walking style is distilled into a loco-manipulation policy via partial adversarial imitation.

B. *Legged Loco-Manipulation*

Early work on legged loco-manipulation methods relied on model-based whole-body control over known dynamics [21], [22], [23], while recent learning-based approaches have demonstrated whole-body coordination across humanoid and quadrupedal platforms through deep controllers [2], force

tracking [3], trajectory optimization [24], teleoperation imitation [25], and residual control [26]. Manipulating large objects with unactuated degrees of freedom and partially observed dynamics, such as carts with passive wheels, remains particularly challenging due to intermittent contacts and unmodeled frictional effects. Existing approaches address this with various methods, including explicit online planning [27], human demonstration priors [28], or combining model-based control with RL [29]. In contrast, our method learns a single end-to-end policy without planning, demonstrations, or a model, instead regularizing locomotion style using a partial adversarial motion prior derived from a reference policy.

C. *Adversarial Imitation Learning*

High quality, deployable controllers for loco-manipulation require a large amount of expert reward tuning or expert reference data. Adversarial imitation learning methods such as GAIL [30] leverage expert demonstrations to reduce the need for hand-crafted rewards by learning a discriminator-based training signal to match the policy and expert state-action distributions.

Building on this discriminator-based formulation, Adversarial Motion Priors (AMP) [7] enables adversarial imitation from state-only information (e.g., state transitions) rather than requiring expert actions and has been widely adopted for learning skills in character control [31], [32], locomotion [33], [34], [35], and whole-body control [36], [37] domains.

Unlike these existing works, our methodology incorporates *partial AMP*, where only a selected subset of the reference agent’s joint state is imitated, and the discriminator and policy operate in the corresponding subset of the target agent’s state rather than the complete state. The most relevant comparison to our work is WASABI [38], where they leverage approximate demonstrations and reduced state information for learning agile behaviors. Our method, on the other hand, is more aligned with hierarchical control, where we separate the learning of a high quality locomotion policy from the manipulation policy learning by using partial state information.

III. LEARNING ROBUST LOCO-MANIPULATION USING PARTIAL ADVERSARIAL MOTION PRIOR

We propose a framework for learning a robust loco-manipulation policy using partial adversarial learning. Our platform is a legged manipulator consisting of a WidowX AI arm [39] mounted on a Unitree Go2 quadruped [40], tasked with pushing a kid-sized shopping cart [41].

The training procedure is divided into two stages. First, we learn a robust, cyclic, and symmetric locomotion reference policy with extensive domain and terrain randomization. Second, we train the loco-manipulation policy while self-imitating only the lower-body reference motions via partial adversarial motion imitation. Terrain randomization is removed in this stage, as uneven terrain is incompatible with stable cart pushing. An overview of the framework is shown in Fig. 2.

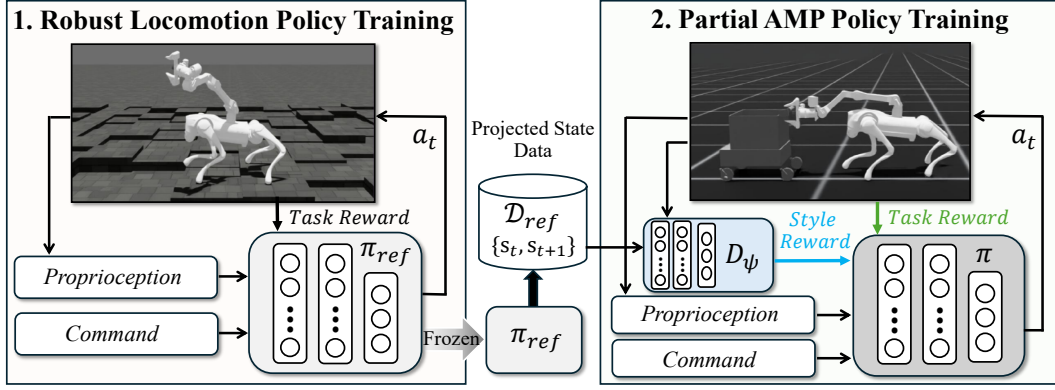


Fig. 2: **Architecture of the proposed framework.** Training is performed in two stages. In stage 1, a robust locomotion reference policy π_{ref} is trained on rough terrain. The resulting policy generates projected state transitions $\mathcal{D}_{\text{ref}} = \{s_t, s_{t+1}\}$ that encode stable locomotion behaviors. In stage 2, we train the loco-manipulation policy using partial adversarial motion priors, where \mathcal{D}_{ref} is used as the reference data for the discriminator to provide a style reward. By imitating only the lower-body motions, the policy maintains stable locomotion while allowing flexible manipulation for cart pushing.

A. Background: Markov Decision Process

We formulate loco-manipulation as a Markov Decision Process (MDP) [42], defined by (S, A, f, r, γ) , where S and A denote the state and action spaces, f the transition function, r the reward function, and γ the discount factor. The goal of reinforcement learning is to find parameters θ for $\pi_\theta(a|s)$ that maximize the expected discounted return

$$J(\theta) = \mathbb{E}_{\tau \sim \pi_\theta} \left[\sum_{t=0}^{T-1} \gamma^t r(s_t, a_t) \right], \quad (1)$$

where $\tau = (s_0, a_0, s_1, \dots)$ denotes a trajectory induced by the policy.

When the full state is not observable, the problem becomes a Partially Observable MDP (POMDP) [43], defined by $(S, A, O, f, \Omega, r, \gamma)$, where O is the observation space and $\Omega : S \rightarrow O$ is the observation function. At each step the agent receives an observation $o_t = \Omega(s_t)$ instead of the true state. In practice, randomized but unobserved environment parameters augment the true state, making the problem partially observable even when the robot's configuration is fully sensed.

B. Robust Locomotion Policy for Motion Prior Generation

Learning a stable and robust locomotion policy that can handle multiple speeds and gait patterns is challenging, particularly when the underlying physics parameters are unknown, and the policy relies solely on proprioceptive observations. To improve robustness, training typically incorporates extensive terrain and dynamics randomization. Because these variations are not directly observable, we formulate the problem as a POMDP, where the policy receives a partial observation o_t instead of the full system state s_t at each control step.

Observation. The policy receives an observation vector $o_t \in \mathbb{R}^{77}$ defined as

$$o_t = [\mathbf{q}_t, \dot{\mathbf{q}}_t, \mathbf{g}_t, \omega_t, \bar{\mathbf{v}}_t, \bar{\omega}_t, \bar{\beta}_t, \bar{\mathbf{p}}_t^{\text{ee}}, \bar{\mathbf{q}}_t^{\text{ee}}], \quad (2)$$

where \mathbf{q}_t and $\dot{\mathbf{q}}_t$ denote the joint angles and joint velocities, respectively. The IMU measurements consist of the

projected gravity vector $\mathbf{g}_t \in \mathbb{R}^3$ expressed in the robot base frame and the base angular velocity $\omega_t \in \mathbb{R}^3$ measured by the gyroscope. The remaining components correspond to command inputs: $\bar{\mathbf{v}}_t$ is the desired base linear velocity, $\bar{\omega}_t$ is the desired base angular velocity, $\bar{\beta}_t$ is the heading command, and $\bar{\mathbf{p}}_t^{\text{ee}}$ and $\bar{\mathbf{q}}_t^{\text{ee}}$ are the end-effector position and orientation command specified relative to the robot base frame. Given the observation o_t , the reference policy π_{ref} outputs target joint angles for both the leg and arm joints, i.e., $a_t \sim \pi_{\text{ref}}(a | o_t)$. Specific observation and command configurations are summarized in Tables I and II.

Reward. The reward function for training π_{ref} encourages stable locomotion while accurately tracking commanded base velocity, heading, and end-effector targets and penalizes jerky or inefficient motions. The reward function is computed as

$$r = r_{\text{tracking}} + r_{\text{regularization}} + r_{\text{gait shaping}} + \mathbb{I}_{\text{term}} \quad (3)$$

where

$$r_{\text{tracking}} = e^{\|\bar{\mathbf{v}} - \mathbf{v}^{xy}\|^2} + e^{(\bar{\omega} - \omega)^2} + e^{(\bar{\beta} - \beta)^2} + e^{\|\bar{\mathbf{p}}^{\text{ee}} - \mathbf{p}^{\text{ee}}\|_1} + e^{-d_{\text{rot}}(\bar{\mathbf{q}}^{\text{ee}}, \mathbf{q}^{\text{ee}})} \quad (4)$$

$$r_{\text{regularization}} = -\left(\|\dot{\mathbf{a}}\|^2 + \|\boldsymbol{\tau}\|^2 + \|\ddot{\mathbf{q}}\|^2 + \|\dot{\mathbf{q}}\|^2 + W + \sum ([\min(\mathbf{q} - \mathbf{q}^{\text{low}}, 0)]^2 + [\max(\mathbf{q} - \mathbf{q}^{\text{high}}, 0)]^2) \right) \quad (5)$$

$$r_{\text{gait shaping}} = -\|\mathbf{q}^{\text{hip}}\|^2 + e^{\|\mathbf{g}\|^2} + e^{(h-0.31)^2} - \left(\sum (|\mathbf{q}^t - 0.5| - 0.4)^2 + (|\mathbf{q}^c + 1.86| - 0.3)^2 \right) - \|\mathbf{f}^f\| - \sum_{\text{legs}} (|\mathbf{q} - \mathbf{q}^d|) \mathbb{I}_{\bar{\mathbf{v}}} \quad (6)$$

where $d_{\text{rot}}(\cdot, \cdot)$ denotes the orientation distance between two quaternions, \mathbf{q}^c are the calf joints, \mathbf{q}^t are the thigh joints, \mathbf{q}^d is the default joint angle, \mathbf{q}^{low} and \mathbf{q}^{high} are the minimum and maximum joint angles, W is the mechanical power, h is the base height, \mathbf{f}^f is the foot contact force, \mathbb{I}_{term} indicates early termination, and $\mathbb{I}_{\bar{\mathbf{v}}}$ indicates whether the commanded velocity is greater than 0.1.

TABLE I: Observation Specifications.

Observation	Noise Range
Base angular velocity	$[-0.20, 0.20]$
Projected gravity	$[-0.05, 0.05]$
Base velocity command	$[-0.10, 0.10]$
Heading command	$[-0.10, 0.10]$
End-effector pose command	$[-0.05, 0.05]$
Relative joint positions	$[-0.02, 0.02]$
Relative joint velocities	$[-1.50, 1.50]$
Previous action	None

TABLE II: Command ranges for reference locomotion policy.

Command	Range
$\bar{\mathbf{v}}_x$ (Global Velocity)	$[0.0, 0.0] \cup [0.1, 1.0]$
$\bar{\mathbf{v}}_y$ (Global Velocity)	$[0.0]$
$\bar{\omega}$ (Angular velocity)	Computed as error correction
$\bar{\beta}$ (Heading Target)	Computed as Error correction
$\bar{\mathbf{p}}_x^{\text{ee}}$ (EE position)	$[0.1, 0.6]$
$\bar{\mathbf{p}}_y^{\text{ee}}$ (EE position)	$[-0.4, 0.4]$
$\bar{\mathbf{p}}_z^{\text{ee}}$ (EE position)	$[0.15, 0.4]$
$\bar{\mathbf{q}}_{\text{roll}}^{\text{ee}}$ (EE orientation)	$[\pi/2]$
$\bar{\mathbf{q}}_{\text{pitch}}^{\text{ee}}$ (EE orientation)	$[-0.1, 0.1]$
$\bar{\mathbf{q}}_{\text{yaw}}^{\text{ee}}$ (EE orientation)	$[0.0]$

State Data Construction. After convergence, we roll out π_{ref} to collect a dataset of state transition pairs

$$\mathcal{D}_{\text{ref}} = \{(s_t^{\text{ref}}, s_{t+1}^{\text{ref}})\}_{t=1}^{T-1}, \quad (7)$$

where s_t^{ref} denotes the state at time step t generated by the reference policy. This dataset captures the locomotion dynamics induced by π_{ref} and serves as reference motion data for partial adversarial imitation training.

C. Loco-Manipulation Policy with Partial Adversarial Motion Priors

In the second stage, we train a loco-manipulation policy π assuming reliable cart position estimation. We leverage (i) a task reward designed for the cart-pushing objective and (ii) a style reward derived from a learned partial adversarial motion prior. To obtain a compact style reward, we adopt the Adversarial Motion Prior (AMP) framework [7], which trains a classifier to distinguish between reference motion data and synthesized motion. The locomotion policy obtained in the first stage is used as the reference motion. Note that we imitate reference state trajectories rather than action trajectories, since our goal is to preserve the locomotion style while allowing the actions to adapt to the additional cart-pushing task.

In standard AMP, the discriminator is trained using a full motion representation of both the reference motion and the motion generated by the learned policy. In our setting, however, forcing the policy to match the full reference state would unnecessarily constrain manipulation, since arm and end-effector states that are optimal for locomotion are not necessarily compatible with reaching and maintaining contact with the cart handle.

We therefore introduce *partial AMP*, in which only a subset of the reference agent’s state is imitated. Concretely, we define a projection function $\phi(\cdot)$ that maps the full

state s_t to a lower-dimensional representation capturing only locomotion-relevant information. In our setting, $\phi(s_t)$ encodes the base motion together with lower-body joint kinematics, including the base angular velocity and the relative joint positions and velocities of the leg joints (hips, thighs, and calves). Manipulation-specific components, such as arm joint states and end-effector states, are excluded so that the adversarial objective regularizes locomotion style while allowing the upper body to adapt to the cart-pushing task. The discriminator is trained on projected state tuples $(\phi(s_t), \phi(s_{t+1}))$, ensuring that the imitation signal constrains only the base and lower-body motion.

We train a discriminator $D_\psi(s)$ using a least-squares adversarial objective [44], where reference transitions are labeled +1 and policy-generated transitions are labeled -1. The training objective is as follows:

$$\begin{aligned} \arg \min_{\psi} \mathbb{E}_{(s,s') \sim \mathcal{D}_{\text{ref}}} [(D_\psi(\phi(s), \phi(s')) - 1)^2] \\ + \mathbb{E}_{(s,s') \sim \pi_\theta(s,a)} [(D_\psi(\phi(s), \phi(s')) + 1)^2] \\ + \frac{w_{gp}}{2} \mathbb{E}_{(s,s') \sim \mathcal{D}_{\text{ref}}} [\|\nabla_{\psi} D_\psi(\phi(s), \phi(s'))\|^2], \end{aligned} \quad (8)$$

where the first term encourages the discriminator to output +1 for reference transitions, the second term encourages it to output -1 for policy-generated transitions, and the third term penalizes large parameter gradients of the discriminator on reference data. This parameter-gradient regularization acts as an additional stabilizer early in training by discouraging excessively sharp discriminator updates and reducing overfitting to the reference dataset [45]. The discriminator output is converted into a style reward that encourages the target policy’s projected transitions to match the reference distribution.

The final loco-manipulation policy is trained using the weighted sum of r_{style} and r_{task} . Each term is defined as follows:

$$r_{\text{style}}(s_t, s_{t+1}) = \max[0, 1 - 0.25(D_\psi(\phi(s), \phi(s_{t+1})) - 1)^2], \quad (9)$$

$$\begin{aligned} r_{\text{task}} = r_{\text{tracking}} + r_{\text{regularization}} \\ - \|\mathbf{q}^{\text{hip}}\|^2 - \|\mathbf{f}^{\text{f}}\| - (v^z)^2 + e^{-40q^{\text{grip}}} \\ - \sum_{\text{legs}} (|\mathbf{q} - \mathbf{q}^{\text{d}}|) \mathbb{I}_{\mathbf{v}} - \sum_{\text{feet}} \|\mathbf{v}\|_2 + \mathbb{I}_{\text{cart}} + \mathbb{I}_{\text{term}} \end{aligned} \quad (10)$$

where \mathbb{I}_{cart} indicates cart height violation. The weights for the style reward and task reward are 1.75 and 1.0, respectively.

We use a curriculum learning strategy for cart loco-manipulation. Training starts with straight-line cart pushing using short episodes for stable contact learning, followed by curved-path cart-turning with longer episodes to handle more complex coordination.

IV. TRAJECTORY FOLLOWING VIA FEEDBACK CONTROL

To enable long-horizon path following for cart pushing, we employ a high-level feedback controller that generates path-following commands for the low-level loco-manipulation policy. Specifically, we use the Stanley controller [46], a

TABLE III: Domain randomization parameters for reference locomotion policy training.

Category	Parameter	Range	Type
Contact material	Static friction	[0.4, 1.2]	Absolute
	Dynamic friction	[0.2, 1.0]	Absolute
	Restitution	[0.0, 0.2]	Absolute
External disturbance	Base force (per axis)	[-10.0, 10.0] N	Absolute
	Base torque (per axis)	[-2.0, 2.0] Nm	Absolute
Dynamics	Link masses	[0.9, 1.1]	Scale
	Joint stiffness (P gain)	[0.9, 1.1]	Scale
	Joint damping (D gain)	[0.9, 1.1]	Scale
Initial state	Base position (x, y)	± 0.05 m	Offset
	Base yaw	± 0.1 rad	Offset
	Base linear vel. (x, y)	± 0.05 m/s	Offset
	Joint positions	± 0.1 rad	Offset
	Joint velocities	± 0.1 rad/s	Offset

TABLE IV: Terrain randomization configuration.

Type	Prop.	Param	Range
Grid boxes	0.42	Height	0.05–0.10 m
Rough terrain	0.24	Noise amp.	0.02–0.10 m
Sine waves	0.17	Wave amp.	0.02–0.08 m
Pyramids	0.17	Slope grade	0.0–0.2

widely adopted method for autonomous driving, to compute a commanded forward velocity \bar{v}_x and yaw rate $\bar{\omega}$ at each control step.

The reference path is represented as a differentiable planar curve in the world frame. The target forward velocity is determined using a heuristic that reduces speed when tracking errors increase or when the path curvature κ is large. At each control step, the controller finds the closest point on the path to the current cart position and computes the cross-track error e_{tr} and heading error e_{head} . The target yaw rate is computed using the standard Stanley control law

$$\omega_{target} = -k_{\theta}e_{head} - \arctan\left(\frac{k_e e_{tr}}{v_{target}}\right), \quad (11)$$

where k_{θ} and k_e are controller gains. Finally, the target velocity and yaw rate are smoothed and clipped before being passed to the low-level policy as commands. Additional implementation details follow the standard Stanley controller formulation in [46].

V. EXPERIMENTS

A. Experimental Design

We study cart loco-manipulation in which the Unitree Go2 + WidowX AI pushes a shopping cart along a predefined path while maintaining continuous contact with the handle. The task is executed by a two-level controller: a high-level Stanley path-following controller that generates the commanded cart linear velocity and yaw rate, and a learned policy that outputs joint position targets to track these commands. The policy runs at 60 Hz using joint position targets while the simulation runs at 240 Hz.

The policies are trained using Proximal Policy Optimization (PPO) [47] in massively parallelized IsaacLab simulation

with 2048 environments. Both the actor and critic are multi-layer perceptrons with hidden sizes [512, 256, 128]. We use a learning rate of 1×10^{-4} , discount factor $\gamma = 0.99$, and clipping parameter 0.2. Training converges in approximately two days on a single RTX 2070 SUPER. Domain and terrain randomization parameters are summarized in Tables III and IV, and latent environment parameters are re-sampled at every episode reset.

We train several variants under identical environment configurations and PPO hyperparameters:

- **No AMP:** A single-stage PPO loco-manipulation policy trained only with the task reward, without any imitation or style regularization.
- **Partial AMP (ours):** A loco-manipulation policy trained with the proposed partial adversarial motion prior, where the AMP discriminator operates on a projection of the state to preserve lower-body motion style.
- **Full AMP:** A loco-manipulation policy trained with a standard AMP objective applied to the full robot state, including both arm and end-effector states.
- **Hierarchical Policy:** A modular baseline that uses the learned locomotion policy for lower-body control, while a separate policy learns residual arm actions for loco-manipulation. The lower-body actions are fixed by the locomotion policy and only the arm actions are learned for the cart-pushing task.

B. Simulation Experiments

Table V and Fig. 3 compare the performance of the proposed and baseline methods in both IsaacLab and MuJoCo environments. The cart loco-manipulation task requires coordinating stable locomotion and accurate manipulation and is trained with a large number of reward terms. While all methods achieve high task success in the training environment (IsaacLab), they exhibit noticeably different qualitative motion patterns, leading to substantial differences in sim-to-sim transfer performance (MuJoCo). In summary, Partial AMP produces the most consistent and stable behaviors across environments.

In IsaacLab, all methods achieve high survival rates (approximately 97–100%) and successfully perform the task. No AMP achieves low tracking errors but typically exhibits a bounding gait with less stable end-effector motion. In contrast, Partial AMP produces a more regular trotting gait with improved end-effector stability. Full AMP tends to overfit to the arm states observed during training, often keeping the arm close to the base, resulting in unstable contact behaviors. The hierarchical policy achieves reasonable task performance but shows limited coordination between locomotion and manipulation due to the fixed lower-body policy.

After transfer to MuJoCo, performance differences become significantly larger. The most common failure mode across methods is loss of contact between the gripper and the cart handle, making stable end-effector motion critical for successful transfer. Overall, Partial AMP achieves the highest survival rate (94.4%) and the lowest tracking errors

TABLE V: Baseline Comparisons with 95% Confidence Interval.

Env	Method	Survival Rate (%)	Lin Vel Error	Ang Vel Error	Heading Error	EE Pos Error	EE Ori Error
IsaacLab	No AMP	96.8 ± 0.7	0.041 ± 0.001	0.041 ± 0.001	0.028 ± 0.000	0.020 ± 0.000	0.853 ± 0.006
	Partial AMP (ours)	99.9 ± 0.1	0.045 ± 0.000	0.085 ± 0.001	0.035 ± 0.001	0.038 ± 0.000	0.293 ± 0.001
	Full AMP	97.2 ± 0.7	0.070 ± 0.003	0.072 ± 0.003	0.047 ± 0.003	0.027 ± 0.001	0.827 ± 0.005
	Hierarchical RL	97.5 ± 0.7	0.088 ± 0.005	0.092 ± 0.002	0.110 ± 0.001	0.039 ± 0.001	0.338 ± 0.002
MuJoCo	No AMP	63.6 ± 4.2	0.332 ± 0.029	0.108 ± 0.007	0.071 ± 0.006	0.150 ± 0.017	0.764 ± 0.026
	Partial AMP (ours)	94.4 ± 1.0	0.156 ± 0.009	0.099 ± 0.007	0.052 ± 0.003	0.082 ± 0.005	0.465 ± 0.018
	Full AMP	31.6 ± 4.1	0.406 ± 0.022	0.158 ± 0.010	0.206 ± 0.022	0.251 ± 0.017	0.886 ± 0.034
	Hierarchical RL	66.0 ± 4.2	0.491 ± 0.020	0.170 ± 0.010	0.200 ± 0.013	0.191 ± 0.012	0.424 ± 0.015

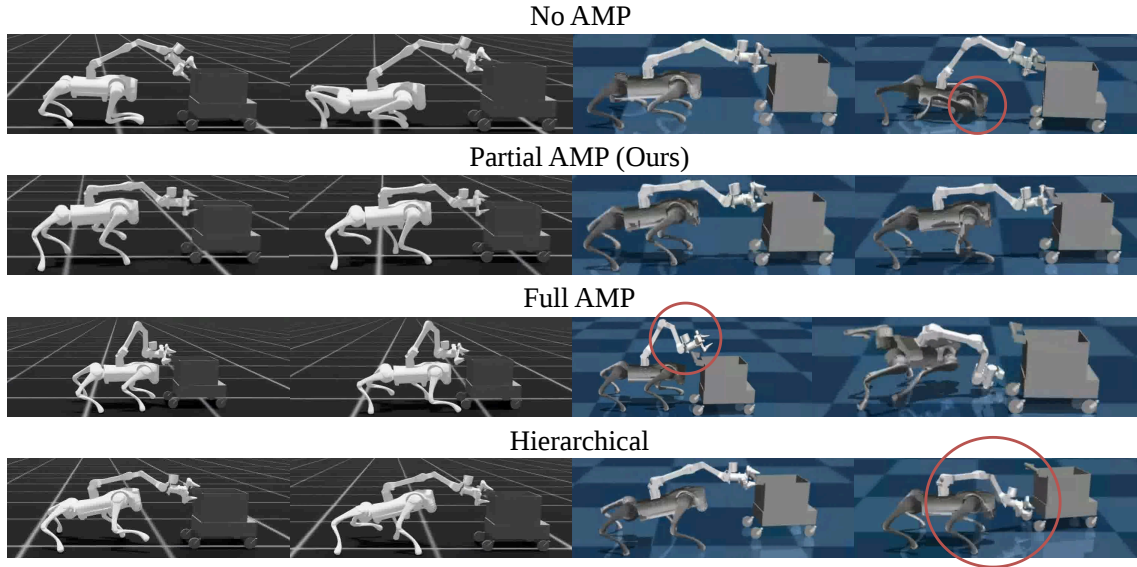


Fig. 3: **Sim-to-Sim Qualitative Comparison.** Depicted on the left is the policy deployed in the source simulator, IsaacSim, and on the right is the target simulator, MuJoCo. Our policy, partial AMP, demonstrates robustness when transferred, showcasing steady locomotion and end effector stability. On the other hand, the baselines are shown with their most common failure points. The No AMP baseline demonstrates feet slip, causing the head to collide with the ground. The Full AMP baseline demonstrates overfitting to the reference manipulator position instead of focusing on end effector tracking, which causes the end effector to slip off the handle. In hierarchical AMP, the robot adopts a conservative stance to prevent falling, resulting in high velocity tracking errors due to the lack of cart pushing.

by producing stable trotting motions and consistent end-effector behavior. No AMP achieves a substantially lower survival rate (63.6%), reflecting the limited robustness of reward-only training due to its less stable bounding-like gait. Full AMP performs worst overall (31.6%), as constraining the full-body motion leads to overly restricted arm behaviors and unstable end-effector motion (Fig. 3, third row). The hierarchical policy achieves intermediate performance (66.0%) but remains less stable, since the fixed locomotion policy cannot adapt when manipulation errors occur.

C. Robustness

To evaluate the robustness of the learned policies in a sim-to-sim transfer setting, we conducted stress tests across various physical parameters. Specifically, the controllers were evaluated against variations in four environmental properties: slide friction (ranging from 0.0 to 2.0), robot mass (scaled from 0.5 to 1.5), cart mass (scaled from 0.5 to 1.5), and wheel damping (ranging from 0.0 to 0.02). Each parameter was evaluated with 50 trials in MuJoCo, while all other parameters remained randomized. A particular parameter was considered successful if the policy achieved a mean survival

rate of at least 30% and maintained a mean linear velocity tracking error of 0.5 or less.

The empirical results are illustrated in Fig. 4. The proposed Partial AMP framework exhibits the best robustness across all parameter variations. No AMP demonstrates acceptable performance but is less resilient than Partial AMP under significant environmental shifts. Conversely, both the Full AMP and Hierarchical baselines fail to satisfy the success criteria under all tested conditions. The failure modes for these baselines are distinct: Full AMP predominantly suffers from premature episode termination and substantial tracking errors, whereas the Hierarchical policy avoids falling but yields excessively high velocity tracking errors, indicating an inability to actually push the cart. Furthermore, Partial AMP provides the most stable loco-manipulation behavior under dynamic variations.

D. Path Tracking

To evaluate long-horizon path-following capabilities, we tested the combined performance of the high-level feedback controller introduced in Section IV and the learned low-level Partial AMP policy. The integrated system was evaluated

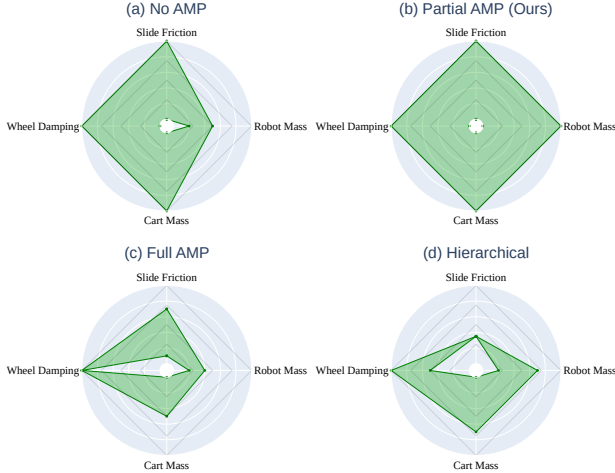


Fig. 4: **Robustness evaluation across environmental variations.** The shaded regions represent the parameter space where each policy satisfies the success criteria (survival rate $\geq 30\%$ and linear velocity error ≤ 0.5).

on three representative continuous trajectories: BeatPath, RiverPath, and SincPath. To rigorously assess the controller’s ability to recover and adjust, environmental domain randomization was applied and the initial conditions of the robot were randomly sampled from a buffer of ≥ 8000 states.

The empirical path-following results are illustrated in Fig. 5. Across these varied spatial profiles, the combined framework demonstrated highly accurate tracking. Specifically, the mean cross-track errors (averaged over five runs) are 0.1238 m for BeatPath (Fig. 5a), 0.0112 m for RiverPath (Fig. 5b), and 0.0885 m for SincPath (Fig. 5c). We observe two primary sources of tracking error. First, initial deviations occur because the robot does not start exactly on the desired path due to the randomized initialization; however, the high-level controller successfully and rapidly compensates to converge onto the target trajectory. Second, further deviations are observed predominantly during sharp turns. These specific errors likely arise because navigating abrupt curves demands angular velocities that exceed the limits of the training distribution (-0.8 to 0.8 rad/s), or they may reflect the inherent physical kinematic limitations of rapidly turning a shopping cart; additionally, the Stanley controller lacks lookahead capability, which limits its ability to anticipate sharp turns.

VI. CONCLUSION

In this work, we presented a novel partial imitation learning framework for robust legged loco-manipulation applied to a cart-pushing task. By employing a partial adversarial motion prior, our approach preserves stable lower-body locomotion styles while allowing the upper body to adapt flexibly to manipulation objectives. Extensive experiments demonstrate that the proposed method outperforms baseline approaches in stability, path-tracking accuracy, and resilience to environmental variations, enabling reliable sim-to-sim transfer.

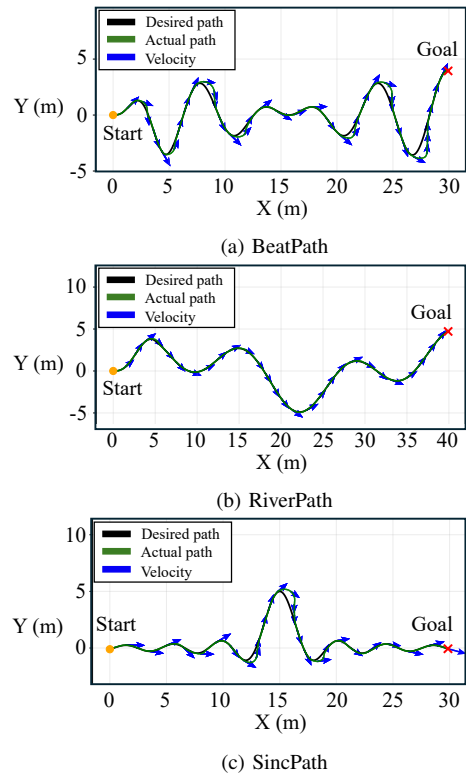


Fig. 5: Individual runs of path-following performance on three representative trajectories. The mean cross-track error (averaged over five runs) is 0.1238 m for BeatPath, 0.0112 m for RiverPath, and 0.0885 m for SincPath, demonstrating accurate path tracking across different trajectory shapes. Blue arrows indicate the instantaneous velocity direction along the motion.

While our proposed Partial AMP framework demonstrates robust loco-manipulation along predefined trajectories, the current system does not incorporate visual feedback. Thus, a natural extension for future work is the integration of vision-based dynamic planning, which would enable legged manipulators to autonomously navigate unstructured environments, avoid obstacles, and generate trajectories in real time. Furthermore, as the primary failure mode observed across all evaluated methods is the unexpected loss of contact between the gripper and the handle, future research should address active contact recovery. Developing policies capable of detecting slip and autonomously executing re-grasping maneuvers will be crucial for deploying these systems in highly reliable, long-horizon real-world applications.

REFERENCES

- [1] M. Liu, Z. Chen, X. Cheng, Y. Ji, R.-Z. Qiu, R. Yang, and X. Wang, “Visual whole-body control for legged loco-manipulation,” 2024. [Online]. Available: <https://arxiv.org/abs/2403.16967>
- [2] Z. Fu, X. Cheng, and D. Pathak, “Deep whole-body control: Learning a unified policy for manipulation and locomotion,” 2022. [Online]. Available: <https://arxiv.org/abs/2210.10044>
- [3] T. Portela, G. B. Margolis, Y. Ji, and P. Agrawal, “Learning force control for legged manipulation,” 2024. [Online]. Available: <https://arxiv.org/abs/2405.01402>
- [4] Z. Fu, Q. Zhao, Q. Wu, G. Wetzstein, and C. Finn, “Humanplus: Humanoid shadowing and imitation from humans,” 2024. [Online]. Available: <https://arxiv.org/abs/2406.10454>
- [5] T. Li, J. Won, S. Ha, and A. Rai, “Fastmimic: Model-based motion imitation for agile, diverse and generalizable quadrupedal locomotion,” 2022. [Online]. Available: <https://arxiv.org/abs/2109.13362>
- [6] J. Li, J. Wu, and C. K. Liu, “Object motion guided human motion synthesis,” *ACM Trans. Graph.*, vol. 42, no. 6, 2023.

- [7] X. B. Peng, Z. Ma, P. Abbeel, S. Levine, and A. Kanazawa, "Amp: adversarial motion priors for stylized physics-based character control," *ACM Transactions on Graphics*, vol. 40, no. 4, p. 1–20, Jul. 2021. [Online]. Available: <http://dx.doi.org/10.1145/3450626.3459670>
- [8] D. Kim, J. D. Carlo, B. Katz, G. Bledt, and S. Kim, "Highly dynamic quadruped locomotion via whole-body impulse control and model predictive control," 2019. [Online]. Available: <https://arxiv.org/abs/1909.06586>
- [9] A. W. Winkler, C. D. Bellicoso, M. Hutter, and J. Buchli, "Gait and trajectory optimization for legged systems through phase-based end-effector parameterization," *IEEE Robotics and Automation Letters*, vol. 3, no. 3, pp. 1560–1567, 2018.
- [10] J. Kim, T. Li, and S. Ha, "Armp: Autoregressive motion planning for quadruped locomotion and navigation in complex indoor environments," in *2023 IEEE/RSJ International Conference on Intelligent Robots and Systems (IROS)*, 2023, pp. 2731–2737.
- [11] D. Youm, H. Jung, H. Kim, J. Hwangbo, H.-W. Park, and S. Ha, "Imitating and finetuning model predictive control for robust and symmetric quadrupedal locomotion," *IEEE Robotics and Automation Letters*, vol. 8, no. 11, p. 7799–7806, Nov. 2023. [Online]. Available: <http://dx.doi.org/10.1109/LRA.2023.3320827>
- [12] J. Tan, T. Zhang, E. Coumans, A. Iscen, Y. Bai, D. Hafner, S. Bohez, and V. Vanhoucke, "Sim-to-real: Learning agile locomotion for quadruped robots," 2018. [Online]. Available: <https://arxiv.org/abs/1804.10332>
- [13] S. Ha, P. Xu, Z. Tan, S. Levine, and J. Tan, "Learning to walk in the real world with minimal human effort," 2020. [Online]. Available: <https://arxiv.org/abs/2002.08550>
- [14] J. Lee, J. Hwangbo, L. Wellhausen, V. Koltun, and M. Hutter, "Learning quadrupedal locomotion over challenging terrain," *Science Robotics*, vol. 5, no. 47, Oct. 2020. [Online]. Available: <http://dx.doi.org/10.1126/scirobotics.abc5986>
- [15] S. Rho, K. Garg, M. Byrd, and S. Ha, "Unsupervised skill discovery as exploration for learning agile locomotion," in *Conference on Robot Learning*. PMLR, 2025, pp. 2678–2694.
- [16] S. Li, Y. Pang, P. Bai, Z. Liu, J. Li, S. Hu, L. Wang, and G. Wang, "Learning agility and adaptive legged locomotion via curricular hindsight reinforcement learning," 2023. [Online]. Available: <https://arxiv.org/abs/2310.15583>
- [17] T. Miki, J. Lee, J. Hwangbo, L. Wellhausen, V. Koltun, and M. Hutter, "Learning robust perceptive locomotion for quadrupedal robots in the wild," *Science Robotics*, vol. 7, no. 62, Jan. 2022. [Online]. Available: <http://dx.doi.org/10.1126/scirobotics.abk2822>
- [18] A. Kumar, Z. Fu, D. Pathak, and J. Malik, "Rma: Rapid motor adaptation for legged robots," 2021. [Online]. Available: <https://arxiv.org/abs/2107.04034>
- [19] M. Byrd, J. Crandell, M. Das, J. Inman, R. Wright, and S. Ha, "Privileged-dreamer: Explicit imagination of privileged information for rapid adaptation of learned policies," in *2025 IEEE International Conference on Robotics and Automation (ICRA)*, 2025, pp. 3640–3646.
- [20] W. Yu, J. Tan, C. K. Liu, and G. Turk, "Preparing for the unknown: Learning a universal policy with online system identification," in *Proceedings of Robotics: Science and Systems*, Cambridge, Massachusetts, July 2017.
- [21] L. Sentis and O. Khatib, "Synthesis of whole-body behaviors through hierarchical control of behavioral primitives," *I. J. Humanoid Robotics*, vol. 2, pp. 505–518, 12 2005.
- [22] C. D. Bellicoso, K. Krämer, M. Stäubli, D. Sako, F. Jenelten, M. Bjelonic, and M. Hutter, "Alma - articulated locomotion and manipulation for a torque-controllable robot," in *2019 International Conference on Robotics and Automation (ICRA)*, 2019, pp. 8477–8483.
- [23] J.-P. Sleiman, F. Farshidian, M. V. Minniti, and M. Hutter, "A unified mpc framework for whole-body dynamic locomotion and manipulation," 2021. [Online]. Available: <https://arxiv.org/abs/2103.00946>
- [24] F. Liu, Z. Gu, Y. Cai, Z. Zhou, H. Jung, J. Jang, S. Zhao, S. Ha, Y. Chen, D. Xu, and Y. Zhao, "Opt2skill: Imitating dynamically-feasible whole-body trajectories for versatile humanoid loco-manipulation," 2025. [Online]. Available: <https://arxiv.org/abs/2409.20514>
- [25] H. Ha, Y. Gao, Z. Fu, J. Tan, and S. Song, "Umi on legs: Making manipulation policies mobile with manipulation-centric whole-body controllers," 2024. [Online]. Available: <https://arxiv.org/abs/2407.10353>
- [26] M. Byrd, D. Baek, K. Garg, H. Jung, D. Cho, M. Sorokin, R. Wright, and S. Ha, "Adaptmanip: Learning adaptive whole-body object lifting and delivery with online recurrent state estimation," 2026. [Online]. Available: <https://arxiv.org/abs/2602.14363>
- [27] Y. Ravan, Z. Yang, T. Chen, T. Lozano-Pérez, and L. P. Kaelbling, "Combining planning and diffusion for mobility with unknown dynamics," 2024. [Online]. Available: <https://arxiv.org/abs/2410.06911>
- [28] T. Li, J. Truong, J. Yang, A. Clegg, A. Rai, S. Ha, and X. Puig, "Robotmover: Learning to move large objects from human demonstrations," 2025. [Online]. Available: <https://arxiv.org/abs/2502.05271>
- [29] J. Cheng, D. Kang, G. Fadini, G. Shi, and S. Coros, "Rambo: RL-augmented model-based whole-body control for loco-manipulation," *IEEE Robotics and Automation Letters*, vol. 10, no. 9, pp. 9462–9469, 2025.
- [30] J. Ho and S. Ermon, "Generative adversarial imitation learning," 2016. [Online]. Available: <https://arxiv.org/abs/1606.03476>
- [31] J. Merel, Y. Tassa, D. TB, S. Srinivasan, J. Lemmon, Z. Wang, G. Wayne, and N. Heess, "Learning human behaviors from motion capture by adversarial imitation," 2017. [Online]. Available: <https://arxiv.org/abs/1707.02201>
- [32] Y. Mu, Z. Zhang, Y. Shi, M. Matsumoto, K. Imamura, G. Tevet, C. Guo, M. Taylor, C. Shu, P. Xi, and X. B. Peng, "Smp: Reusable score-matching motion priors for physics-based character control," 2025. [Online]. Available: <https://arxiv.org/abs/2512.03028>
- [33] A. Escontrela, X. B. Peng, W. Yu, T. Zhang, A. Iscen, K. Goldberg, and P. Abbeel, "Adversarial motion priors make good substitutes for complex reward functions," 2022. [Online]. Available: <https://arxiv.org/abs/2203.15103>
- [34] E. Vollenweider, M. Bjelonic, V. Klemm, N. Rudin, J. Lee, and M. Hutter, "Advanced skills through multiple adversarial motion priors in reinforcement learning," 2022. [Online]. Available: <https://arxiv.org/abs/2203.14912>
- [35] J. Wu, G. Xin, C. Qi, and Y. Xue, "Learning robust and agile legged locomotion using adversarial motion priors," *IEEE Robotics and Automation Letters*, vol. 8, no. 8, pp. 4975–4982, 2023.
- [36] Y. Chen, S. Dong, X. Ji, J. Sun, Z. Luo, L. Zhao, J. Zhang, W. Li, J. Ma, B. Xu, Y. Han, Y. Zhao, and P. Lu, "Learning human-like badminton skills for humanoid robots," 2026. [Online]. Available: <https://arxiv.org/abs/2602.08370>
- [37] H. Wang, W. Zhang, R. Yu, T. Huang, J. Ren, F. Jia, Z. Wang, X. Niu, X. Chen, J. Chen, Q. Chen, J. Wang, and J. Pang, "Physhi: Towards a real-world generalizable and natural humanoid-scene interaction system," 2025. [Online]. Available: <https://arxiv.org/abs/2510.11072>
- [38] C. Li, M. Vlastelica, S. Blaes, J. Frey, F. Grimmering, and G. Martius, "Learning agile skills via adversarial imitation of rough partial demonstrations," in *Conference on Robot Learning*. PMLR, 2023, pp. 342–352.
- [39] Trossen Robotics, "WidowX AI Robot Arm." [Online]. Available: <https://www.trossenrobotics.com/widowx-ai>
- [40] Unitree Robotics, "Unitree Go2 Quadruped Robot." [Online]. Available: <https://shop.unitree.com/products/unitree-go2>
- [41] Melissa & Doug, "Shopping Cart Toy - Metal Grocery Wagon." [Online]. Available: <https://www.melissaanddoug.com/products/shopping-cart-toy-metal-grocery-wagon>
- [42] R. S. Sutton and A. G. Barto, *Reinforcement learning: an introduction*, second edition ed., ser. Adaptive computation and machine learning series. Cambridge, Massachusetts: The MIT Press, 2018.
- [43] L. P. Kaelbling, M. L. Littman, and A. R. Cassandra, "Planning and acting in partially observable stochastic domains," *Artif. Intell.*, vol. 101, pp. 99–134, 1998. [Online]. Available: <https://api.semanticscholar.org/CorpusID:5613003>
- [44] X. Mao, Q. Li, H. Xie, R. Y. K. Lau, Z. Wang, and S. P. Smolley, "Least squares generative adversarial networks," 2017. [Online]. Available: <https://arxiv.org/abs/1611.04076>
- [45] L. Mescheder, "On the convergence properties of gan training," 01 2018.
- [46] G. M. Hoffmann, C. J. Tomlin, M. Montemerlo, and S. Thrun, "Autonomous automobile trajectory tracking for off-road driving: Controller design, experimental validation and racing," in *2007 American Control Conference*, 2007, pp. 2296–2301.
- [47] J. Schulman, F. Wolski, P. Dhariwal, A. Radford, and O. Klimov, "Proximal policy optimization algorithms," 2017. [Online]. Available: <https://arxiv.org/abs/1707.06347>